Thixotropy and Yield Stress Behavior in Drilling Fluids
Jason Maxey, Baker Hughes Drilling Fluids

Abstract
Drilling fluids are commonly recognized as complex fluids which exhibit both yield stress behavior and varying degrees of thixotropy. Traditional models for yield stress behavior have been used extensively, with the Bingham plastic model remaining prevalent for description in the field and the Herschel-Bulkley model becoming the standard for computer simulations of fluid behavior. Neither of these models represents the full behavior of drilling fluids, either missing aspects of the shear-thinning behavior or inaccurately predicting the yield stress of the fluids. These errors are exacerbated through variations in measurement techniques by technicians who do not fully appreciate the thixotropic nature of these fluids. An improved understanding of the rheological behavior, in particular the yield and thixotropic nature, of drilling fluids would result in improved models and enhanced drilling performance, thereby reducing drilling costs.

An examination of some typical drilling fluids will be presented. The intertwined effects of thixotropy and yield stress on rheological measurements will be highlighted. These fluids will also be evaluated with traditional yield stress models as well as with several recently proposed models.

Introduction

Drilling fluids have a great deal of responsibility placed on them, not the least of which is the necessity for rheological flexibility during the drilling process. While fluid flow is usually constant during periods of drilling, depending on rate of penetration, drill pipe eccentricity produces uneven flow in the annulus. Dramatic differences in shear rate can be observed in the annular gap when comparing the wider and narrower gaps due to this eccentricity. Because of the potential for loss of solids suspension (specifically weighting agents and drilled cuttings) the fluid must embody both fluid behavior, for ease of pumping, and solid behavior, for suspension of solids. In other words, a drilling fluid must be viscoelastic. Even when pipe eccentricity is minimal, fluid flow is laminar plug flow, with the maximum expected shear rate at the wall being less than 400 s^{-1} (equivalent to ~235-rpm on a Model 35A viscometer). This shear rate quickly drops with distance from the wall, allowing the fluid to structure while flowing and providing another case for the need for a viscoelastic drilling fluid.[1]

The performance of a drilling fluid is strained even further by the intermittent nature of drilling. While drilling ahead, relatively long periods of fluid flow will be interrupted by short periods (usually less than ten minutes) when the fluid is not pumped as a connection is made. During non-drilling activities (tripping pipe, running casing, etc.) the drilling fluid may lie stagnant in the hole for hours or even days. During this period, settling of solids can be especially problematic if the fluid does not have enough structure to support both large and small particulate matter. For these reasons clays, which form associative networks, are used as viscosifiers. They provide both a structural network that suspends solids in low-shear / no-flow situations and are sufficiently shear-thinning to allow pumpability. However, an overly-structured fluid can provide problems as severe as an under-structured fluid. If the fluid builds a sufficiently strong structure, the stress required to break the structure (by tripping pipe, initiating pump flow, etc.) and initiate flow will become excessively high, resulting in tremendous pressure surges and the likelihood of fracturing the formation. The balance between minimizing swab and surge pressures without allowing barite sag can be difficult to maintain in fluids that are thixotropic and exhibit a yield stress.

Thixotropy and Yield Stress

It is well understood that drilling fluids are time-dependant materials; that is, they exhibit thixotropic tendencies. It has also been observed that drilling fluids do not flow unless subjected to a certain load (stress); that is, they are yield stress materials. Yield stress fluids can be defined as fluids that can support their own weight to a certain extent, *i.e.* they can support shear stresses without flowing as opposed to Newtonian fluids. Thixotropy can be defined as a reversible decrease of viscosity of the material in time when a material is made to flow. Though thixotropy and yield stress are usually considered as separately phenomena, they show a tendency toward appearing in the same fluid. In addition, they are indeed believed to be caused by the same fundamental physics. The same microstructure present in a fluid that resists large rearrangements (which is responsible for the yield stress), when broken by flow, is believed to be the origin of thixotropy.[2]

A common method for evaluating the thixotropic nature of a material is the thixotropic loop test. In this test, the material is pre-sheared to thoroughly break down any existing structure in the fluid and often allowed a rest period to rebuild structure (providing a common starting point for tests). The shear rate

is then swept from zero up to a maximum rate (up-sweep curve) and then swept down to rest (down-sweep curve). If the structure of the sample recovers during the rest period after pre-shear and is subsequently broken again during the measurements, the up-shear curve will run above the down-shear curve, producing a loop on the stress/rate plot which signifies a positively thixotropic material. In general, drilling fluids tend to exhibit positive thixotropy. If that structure does not recover at rest after pre-shearing, application of a sufficiently high shear rate may result in a shear-induced increase in viscosity. This would reverse the loop, with the down-sweep curve above the up-sweep curve, in a negatively thixotropic loop. Negative thixotropy is usually defined as a system which thickens at high rates and retains its thickened condition at rest in which viscosity drops after application of a low shear. A third possible behavior exists, called rheopexy, in which structural recovery is accelerated by shearing. This is differentiated from negative thixotropy in that it requires certain shearing to recover structure but that stress does not decrease after a reduction in shear.[3]

Determination of Thixotropy and Yield Stress

Yield stress fluids are commonly found in many applications, including foods (mayonnaise), cosmetics, hygiene (shaving creams and toothpaste) as well as those common to the drilling industry (muds and cement). The most common conception of a yield stress fluid is that of a discontinuous model where flow occurs only above a certain stress (σ_y). For such a model, viscosity increases to infinite as strain rate decreases. Despite the abundance of potential models and experimental methods for determination of yield stress, a definitive method has yet to arise. Different tests often result in different yield stress values, depending on the measurement geometry and experimental protocol. It has been demonstrated that a variation in measured yield stress of greater than one order of magnitude can arise from different experimental methods.[2] These variations arise from phenomenon such as wall slip, shear banding, short test periods, and variations in the definition of what point in a test constitutes the yielding of the fluid, among others.

The same variation is found to be true of models used to determine yield stress. Many different models have been employed for drilling fluids, some based on the assumption of a yield stress (*yield stress models*) and some which do not explicitly consider a yield stress (*viscosity models*). The most common of these are detailed in Table 1 and Table 2. Among the viscosity models, the power law model is the simplest and most widely applied. However, the power law predicts a uniform flow regime at all rates, unlike the Cross and Carreau models which predict changes from upper shear-thinning to yield stress plateau to lower-Newtonian behavior. When more computing power is available, the Cross and Carreau models are often used, but for quick and simple predictions for hydrodynamic calculations the power law model is still employed.

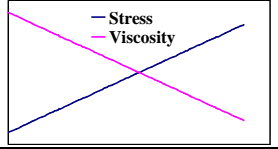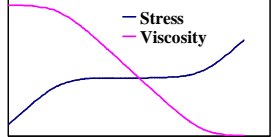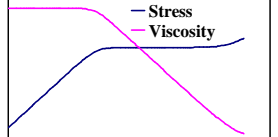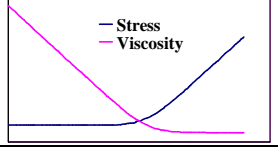**Table 1** Common viscosity models for drilling fluids.

Power Law	$\eta = K\dot{\gamma}^{n-1}$	
Cross	$\eta = \dfrac{\eta_0 - \eta_\infty}{1 + a\dot{\gamma}^n} + \eta_\infty$	
Carreau	$\eta = \dfrac{\eta_0 - \eta_\infty}{\left(1 + a\dot{\gamma}^2\right)^n} + \eta_\infty$	

Table 2 Common yield stress models for drilling fluids.

Bingham Plastic	$\sigma = \sigma_0 + \eta_p\dot{\gamma}$	
Herschel-Bulkley	$\sigma = \sigma_0 + \eta_p\dot{\gamma}^n$	
Casson	$\sqrt{\sigma} = \sqrt{\sigma_0} + \sqrt{\eta_\infty\dot{\gamma}}$	
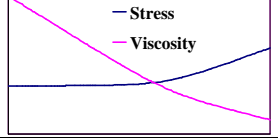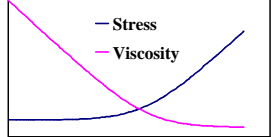
Among the models used for drilling fluids, the Bingham plastic model is by far the most widely used. As a simple linear model, the parameters can be calculated readily and, when using Model 35A data from 600-rpm and 300-rpm, give the plastic viscosity and yield point commonly reported for drilling fluids. However it, too, suffers from the same inflexibility as the power law model; although, the Bingham plastic model does allow for a shear-thinning region and a yield stress region. A commonly used derivative of the power law and Bingham plastic models is the Herschel-Bulkley (H-B) model. As the H-B yield stress approaches zero, the model reduces to the power law; and when n approaches unity, the H-B model reduces to the Bingham plastic form. This model provides a bit more flexibility and, when evaluated over a minimal range of strain rates, does a good job of fitting many drilling fluids. A somewhat better fit is often found from the Casson model, though its complexity makes for difficult fitting.

Complicating the ability of a model to accurately mirror a fluid is the dearth of good data describing the fluid. Typical measurements involve the Model 35A viscometer, which

yields only six data points, two of which are at shear rates greater than what is typically seen in the wellbore and the lowest rates are above the point at which dynamic sag is expected to occur. In addition, the accuracy of the limited amount of data usually available is low, with a combined error from visual measurement and calibration of 1.5° deflection. At 600-rpm, this amounts to only an error of 0.75-cP; however, at 3-rpm this is an error of 150-cP, potentially greater than 20% total error at 3-rpm. Further, because data collection is often rushed, the fluid is not at equilibrium when the measurement is made. The thixotropic nature of drilling fluids causes them to actually structure while flowing[1,2], so lower strain rate data can easily take 1-5 minutes to reach a steady state value. When non-equilibrium data is used in generating a model, a very poor picture of the fluid is painted and predictions based on this data is faulty. The same holds true for gel strength measurements on a Model 35A. If not given sufficient shearing time to break gel structure before proceeding to the next gel strength test, the results of the tests become cumulative and not independent.

Recent Models

It has been noted that, despite the flexibility of some of these models, no single model does a sufficiently good job of predicting the behavior of all types of drilling fluids. Modeling of fluid behavior is of extreme importance to predicting downhole performance, and the lack of a single model that can be consistently applied detracts from the ability to do so accurately.[4] Recently, several models have been developed which attempt to better model the yield stress behavior of fluids and even incorporate structural terms to account for thixotropic behavior. Good use of these models, as with other models, requires more data points than are available from a 6-speed viscometer. However, the increasing use of field-usable viscometers with an extended range of strain rates makes the use of such models more viable. One model, proposed by Mendes and Dutra[5], provides more accurate modeling of experimental data and relative ease of calculating parameters. Their viscosity function (Equation 1) predicts an upper shear-thinning region, a yield stress plateau, and a Newtonian behavior at low shear rates. The type of shear stress and viscosity response to strain rate is shown in Figure 1. From these curves it is easy to estimate the yield stress, σ_0, the zero-shear viscosity, η_0, and the shear-thinning index, n. Using the estimated value for n, K can be quickly calculated as the stress at $\dot{\gamma}=1$ s^{-1} from the power law equation.

$$\sigma = \left(1 - e^{-\eta_0\dot{\gamma}/\sigma_0}\right)\left(\sigma_0 + K\dot{\gamma}^n\right) \qquad (1)$$
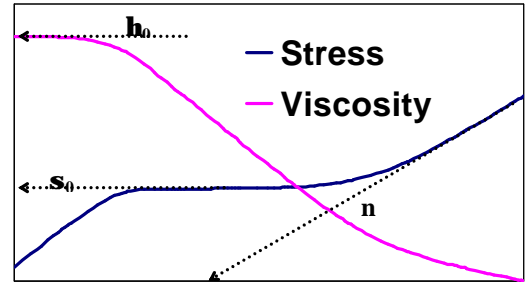
.

Figure 1 Shear stress and viscosity as a function of strain rate as predicted by Equation 1, the Mendes-Dutra viscosity function.

Another recent model, proposed by Møller, Mewis, and Bonn[2], provides a more interesting method for predicting fluid behavior. In their model, they take into account both traditional shear-thinning and yield behavior and add a component that models structural connectivity in the fluid. They begin with three basic assumptions:

1. There exists a structural parameter, λ, that describes the local degree of interconnection of the microstructure.
2. Viscosity increases with increasing λ.
3. For an aging (thixotropic) system at low or zero shear rate, λ increases while the flow breaks down the structure, λ decreases and reaches a steady state value at sufficiently high shear rates.

Based on these assumptions, they developed the following structural evolution equation and viscosity equations.

$$\frac{d\lambda}{dt} = \frac{1}{\tau} - \alpha\lambda\dot{\gamma} \qquad (2)$$

$$\eta = \eta_\infty e^{\beta\lambda} \text{ (Model I)} \qquad (3a)$$

$$\eta = \eta_\infty\left(1 + \beta\lambda^n\right) \text{ (Model II)} \qquad (3b)$$

Here τ is the characteristic time of microstructural build-up at rest, η_∞ the limiting viscosity at high shear rates, and α, β and n are material-specific parameters. Under steady state conditions, using Equation 3b, the stress behavior of a fluid may be modeled as

$$\sigma = \dot{\gamma}\eta_\infty\left(1 + \beta(\alpha\tau\dot{\gamma})^{-n}\right) \qquad (4)$$

which, at high shear rates, yields Newtonian behavior. When $0 < n < 1$, a simple shear-thinning fluid without a yield stress is produced. However, when $n > 1$, a yield stress appears in the model; additionally, a critical stress is predicted below which no steady state shear rate can be achieved and flow is unstable (see Figure 2). It is therefore possible to have a sample of the same thixotropic fluid exhibiting the same viscosity at a given strain rate, but with very different structures[2].
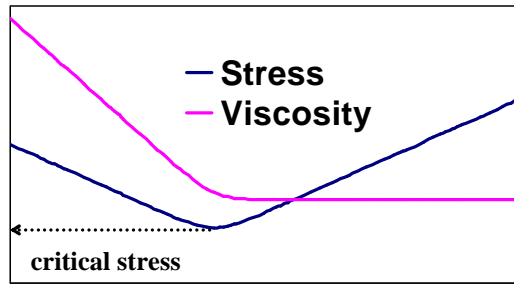
Figure 2 Shear stress and viscosity as a function of strain rate as predicted by Equation 4, for n=2. Illustrated is the critical stress below which flow is unstable.

These two models (Equations 1 and 4) are very different in their suppositions and, as a result, lead to very different predictions. The Mendes-Dutra model (Equation 1) presumes a very high, Newtonian viscosity occurring below the yield stress and that an imposed stress below that yield stress will produce a constant flow of the material. The thixotropy model (Equation 4), on the other hand, predicts unstable flows below the yield stress. If the structural component, λ, is initially small, an applied stress could result in flow which remains measurable for some finite time, but will eventually stop as λ increases. By the thixotropy model, the yield stress should now be defined as the stress below which no permanent flow occurs[2]. This yields another varied method for determination of the "true" yield stress, one that accounts for the structure formed in the fluid rather than being independent of that structure.

Test Fluids and Methods

Four fluids were evaluated in this work, each selected to demonstrate a range of different, yet typical, behaviors of drilling muds. Each of these fluids was tested to evaluate their tendency toward thixotropic behavior and, by various methods, to determine yield stress in the fluid. By way of comparison to the empirical measurements of yield stress, fluid behavior was also modeled to each of the six traditional and two newer models.

Two water-based muds and two oil-based muds were selected for assessment, and are described in Table 3. The water-based fluids have similar pH, identical clay loading, and similar treatments for fluid loss, differing mainly in the deflocculation and final fluid density. The two oil-based fluids have identical densities and oil/water ratios, slightly different organophilic clay concentrations, but are weighted up to final fluid density by different means. None of the tested fluids included drilled solids, which would be expected to increase thixotropic and yield behavior.

Rheological testing was performed on three instruments, an Anton-Paar MCR301 stress-controlled rheometer and a Rheometrics RFS-III strain-controlled rheometer and an OFI-900 viscometer. In general, before testing, all samples were brought to a test temperature of 120°F and then presheared for two minutes at 1022 s^{-1} (600-rpm on a Model 35A viscometer) and the relevant test was run immediately. The time allowed

Table 3 Formulations and Model 35A properties of fluids tested in this study.

	Fluid #1	Fluid #2	Fluid #3	Fluid #4
Base Oil, bbl	--	--	0.55	0.56
Water, bbl	0.92	0.7	--	--
25% CaCl₂ Brine, bbl	--	--	0.16	0.16
Emulsifier, lb/bbl	--	--	12	12
Organophilic Clay #1, lb/bbl	--	--	2.5	1.5
Organophilic Clay #2, lb/bbl	--	--	2.5	1.5
Organic Rheological Modifier , lb/bbl	--	--	2	2
Bentonite, lb/bbl	20	20	--	--
Lignosulfonate, lb/bbl	1	0	--	--
Lignite, lb/bbl	0.5	0.3	--	--
Caustic, lb/bbl	0.75	0.3	--	--
NaCl, bbl	36	--	--	--
Starch, lb/bbl	1	1	--	--
Barite, lb/bbl	50	405	345	262
Ilmenite, lb/bbl	--	--	--	88
Hot Rolled at 150°F, 16-hours				
Mud Weight, lb/gal	10	16	14	14
OWR	--	--	80/20	80/20
Model 35 600-rpm @ 120°F	27	233	58	58
Model 35 300-rpm @ 120°F	18	156	35	33
Model 35 200-rpm @ 120°F	14	124	25	24
Model 35 100-rpm @ 120°F	10	85	16	15
Model 35 6-rpm @ 120°F	6	28	5	5
Model 35 3-rpm @ 120°F	8	24	5	5
Plastic Viscosity, cP	9	77	23	25
Yield Point, lb/100 ft²	9	79	12	8
10-second Gel, lb/100 ft²	7	24	6	8
10-minute Gel, lb/100 ft²	10	46	12	14
30-minute Gel, lb/100 ft²	11	68	13	15

for collection of data points was varied, as was the duration of the rest period after preshearing in which a gel structure was allowed to grow. When possible, a profiled geometry was used to reduce the impact of wall slip on recorded data. For tests performed on the OFI-900 viscometer, two basic set-ups were employed (Table 4), in order to compare the results of a standard oilfield test where time is critical with a test in which time is allowed for steady-state to be achieved in the fluid.

Table 4 Test methodology for viscometric evaluation of drilling fluids.

Test Method A	Test Method B
1. Adjust temperature to 120°F while shearing at 300-rpm (511 s^{-1})	1. Adjust temperature to 120°F while shearing at 300-rpm (511 s^{-1})
2. Preshear at 600-rpm (1022 s^{-1}) for 5-minutes	2. Preshear at 600-rpm (1022 s^{-1}) for 5-minutes
3. Observe deflection at 600, 300, 200, 100, 6, and 3-rpm allowing ***10-seconds per data point***	3. Observe deflection at 600, 300, 200, 100, 6, and 3-rpm allowing ***60-seconds per data point***
4. After the rate sweep, 10-second, 10-minute, and 30-minute gel strengths are tested with the fluid sheared at 600-rpm for ***20-seconds*** prior to each test	4. After the rate sweep, 10-second, 10-minute, and 30-minute gel strengths are tested with the fluid sheared at 600-rpm for ***5-minutes*** prior to each test

Thixotropic Evaluation

Three basic methods were used to compare the thixotropic nature of the test fluids. First used was the thixotropic loop, and results of these can be seen in Figure 3 (for Fluid #2) and Figure 4 (for Fluid #4). In these tests the samples was initially presheared at 1022 s^{-1} for two minutes and the fluid allowed a rest period for structural growth (either 10-seconds or 10-minutes) before the strain rate was swept from 0 s^{-1} to 100 s^{-1} over 450-seconds and then swept back down to 0 s^{-1} over 450-seconds.

For Fluid #2, when only a 10-second gel period was allowed, little thixotropy is evidenced in the fluid. The up-sweep and down-sweep curves are coincidental over much of the test region. However, when a 10-minute gel period is allowed, the up-sweep curve lies decidedly above the down-sweep below ~100 s^{-1}, indicating positive thixotropy. An interesting characteristic in the fluid's behavior is that the up-sweep experiences a stress peak, at ~6 s^{-1}, indicating a start-up resistance to flow which breaks back with increased shear. Also interesting is that the down-sweep of the 10-minute gel test is not coincidental with the down-sweep of the 10-second test, as might be expected. This would seem to indicate that the structure developed during the 10-minute rest period has not been completely broken down by the shearing of this test, despite the duration and high degree of shear the fluid experienced. This may be classified as a strong gel; one that forms a strong associative network that resists breaking under flow.
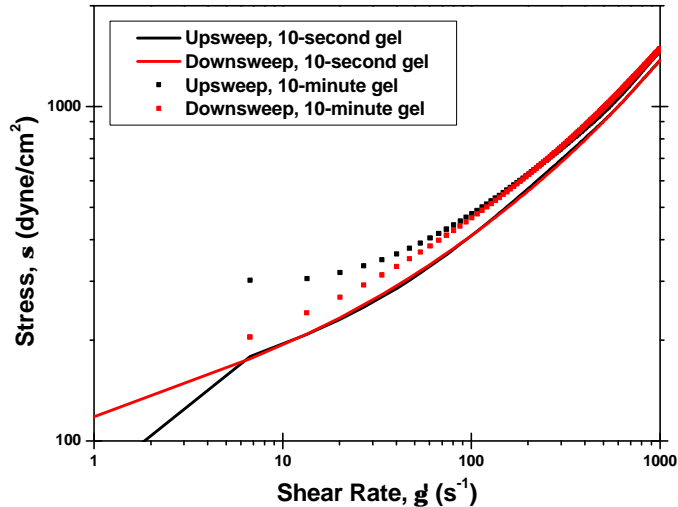

Figure 3 Thixotropic loop at 120°F for Fluid #2, performed after 10-second and 10-minute gel periods, demonstrating the strong thixotropic nature of the drilling fluid.

For Fluid #4, strong thixotropy was evidenced in the fluid in both 10-second and 10-minute gel tests. The up-sweep and down-sweep curves are coincidental only at high rates (> 500-s^{-1}), which may indicate the strength of the thixotropic nature of the fluid. As with Fluid #2, the up-sweep experiences a stress peak which breaks back with increased shear. This peak

is greater in the 10-minute gel test, indicating that the gel structure continued to form after the initial 10-second period. Unlike the results observed with Fluid #2, however, the down-sweep of the 10-minute gel test is coincidental with the down-sweep of the 10-second test. This is indicative that despite strong thixotropy evidenced in Fluid #4, the structure developed is readily broken under shear. This may be classified as a fragile gel; one that forms a weak associative network that breaks easily under flow.
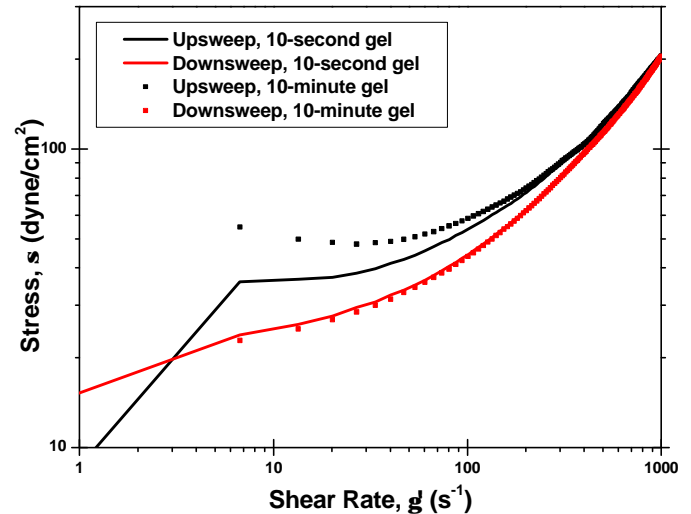

Figure 4 Thixotropic loop at 120°F for Fluid #4, performed after 10-second and 10-minute gel periods, demonstrating the strong thixotropic nature of the drilling fluid coupled with a fragile gel structure.

Another method of examining the thixotropic response of a fluid is through a shear-loading experiment. Here, a low strain rate (1 s^{-1}) is applied to the fluid to observe a base-line viscosity response. The fluid is then sheared at a higher rate (100 s^{-1} for one minute) in order to break down the structure that was intrinsic in the fluid. Finally, the same low strain rate is applied for a long period of time and the stress / viscosity response over time observed. Figure 5 exhibits the results of a shear-loading experiment for Fluid #2. After 25-minutes shearing at 1 s^{-1} the fluid exhibited a viscosity 50% higher than it had in the initial 1 s^{-1} shearing interval. As can be seen, the steady growth of structure resulted in a constant increase in measured viscosity of the fluid. This is very relevant to common practices for fluid evaluation using a Model 35A viscometer, where the preshear history can be vastly different and the structural state of the fluid substantially effects the recorded data. With some muds, as was the case with Fluid #2, data taken at low rates – especially 6-rpm and 3-rpm - can differ greatly depending on the time allowed for the fluid to reach a steady state; indeed, the steady state may not be achieved in a reasonable time period.
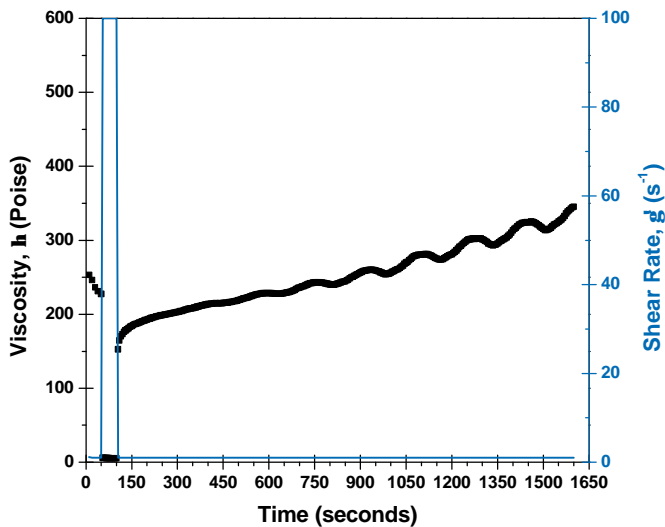
Figure 5 Shear loading test at 120°F for Fluid #2, demonstrating the steady growth of structure under shear.

Because of the expectations for thixotropy influencing test results, particularly at low strain rates, the series of tests described in Table 4 were devised. These tests allow for comparison of the effects of thixotropy on data from oilfield viscometry tests in cases where a test time is minimal (Test Method A) and when time is taken to allow for steady state to be reached in the fluid (Test Method B). The results of these tests for the two water-based fluids (Fluids #1 and #2) are presented in Figure 6. For Fluid #2, there is relatively little difference in the results of the two tests; however, the lower strain rate data for Fluid #1 demonstrates some of the expected differences. Below 100-rpm the recorded stresses (bob
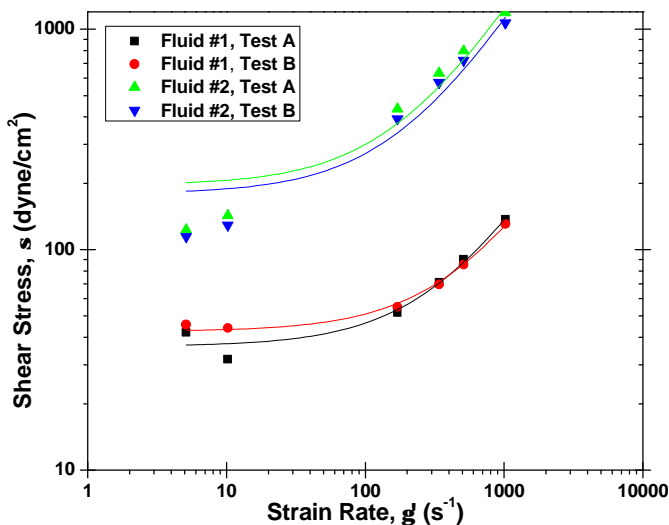
deflections) from Test Method B are consistently greater than those from Method A. Of particular interest is the increase in recorded stress from 6-rpm to 3-rpm in Method A; this is evidence that the fluid is building structure under flow and that a steady state in the fluid has not been achieved when data is taken. By comparison, Method B stresses at 6-rpm and 3-rpm are greater than those for Method A and do not exhibit the up-turn.

Yield Stress Evaluation

The first step in examining the yield stress of the four selected fluids was through modeling using the standard oilfield method. Along with the raw data in Figure 6 is a fit of the 600-rpm and 300-rpm data points to the Bingham plastic model, the common method for calculating Plastic Viscosity and Yield Point in drilling fluids. For Fluid #1 the simple two-point model produces a relatively accurate model of fluid behavior, despite extrapolation to far below the data used in the model. However, Fluid #2 gives a very poor data fit, with the Yield Point from the two-point model over-predicting the yield stress plateau greatly. A fit of the same data using a six-point Bingham plastic model is presented in Figure 7, with better fits seen for Fluid #1. A comparison of the predicted yield stress, σ_0, and plastic viscosity, η_p, are presented in Table 5. As observed graphically, the two-point and six-point fits for Fluid #1 are qualitatively identical, while large differences are observed for Fluid #2. These differences, from simply applying a two-point to a six-point data fit, demonstrate the expectation that better modeling can be achieved through the use of more data. A similar improvement in fits using six-points is also observed for Fluids #3 and #4.
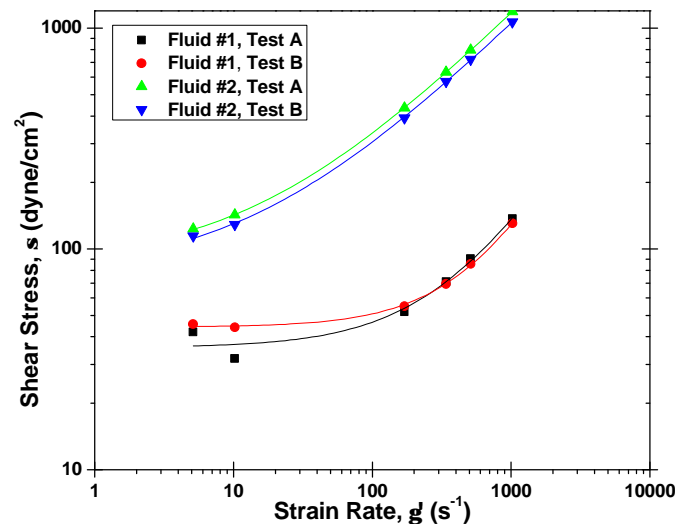

Figure 6 Viscometry results for Fluids #1 and #2 at 120°F when tested by Test Methods A and B and fit by the Bingham plastic model using only the 600-rpm and 300-rpm data.

Figure 7 Viscometry results for Fluids #1 and #2 at 120°F when tested by Test Methods A and B and fit by the Bingham plastic model using all six data points.

Table 5   Yield stress and plastic viscosity from Bingham plastic fits of viscometry data for Fluids #1 and #2, using either 2-points or six-points for fitting.

	2-point Fit Parameters	6-point Fit Parameters
Fluid #1, Test A	$\sigma_Y = 43.4$ dyne/cm^2 $\eta_p = 9.2$ Poise	$\sigma_Y = 36.4$ dyne/cm^2 $\eta_p = 10.0$ Poise
Fluid #1, Test B	$\sigma_Y = 40.0$ dyne/cm^2 $\eta_p = 8.9$ Poise	$\sigma_Y = 42.6$ dyne/cm^2 $\eta_p = 8.5$ Poise
Fluid #2, Test A	$\sigma_Y = 404.9$ dyne/cm^2 $\eta_p = 76.9$ Poise	$\sigma_Y = 195.5$ dyne/cm^2 $\eta_p = 104.3$ Poise
Fluid #2, Test B	$\sigma_Y = 377.4$ dyne/cm^2 $\eta_p = 67.5$ Poise	$\sigma_Y = 179.4$ dyne/cm^2 $\eta_p = 93.3$ Poise

In light of the knowledge that improved and increased data allows for better modeling of a fluid, the four test fluids were characterized for stress / strain rate behavior on the two available rheometers. Flow curves were generated under controlled strain rate and controlled shear stress tests, with the rate sweeps collecting 150 data points between 1200 s^{-1} and 0.001 s^{-1}, allowing 10-seconds per data point. Shear stress controlled tests were conducted so that the three main flow regimes (upper shear-thinning, yield stress plateau, and lower shear-thinning / Newtonian) were observed, collecting 150 data points with between 5-seconds and 100-seconds allowed for equilibration at each stress. The resultant flow curves were then compared to the standard and newer models described above.

Flow curves generated from controlled strain rate tests are exhibited in Figure 8 (for Fluid #2) and in Figure 9 (for Fluid #4). It is interesting to observe that these two fluids present very different responses at low strain rates. The shear stress
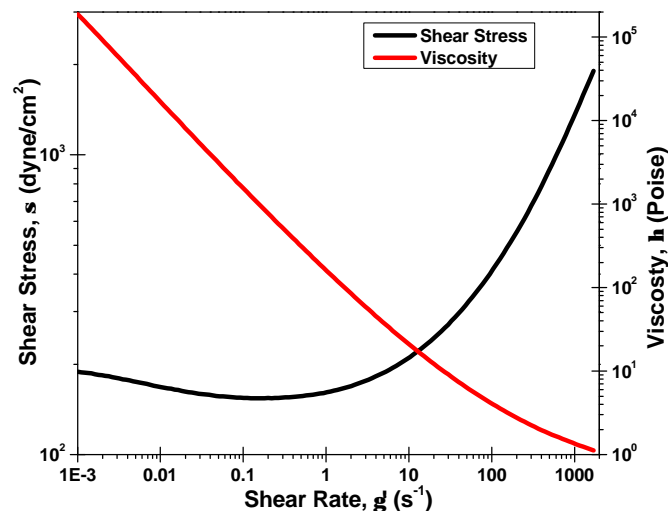
Figure 8   Controlled rate flow curve at 120°F for Fluid #2, demonstrating a behavior similar to that predicted by the thixotropy model for a fluid with a strong structural growth component.
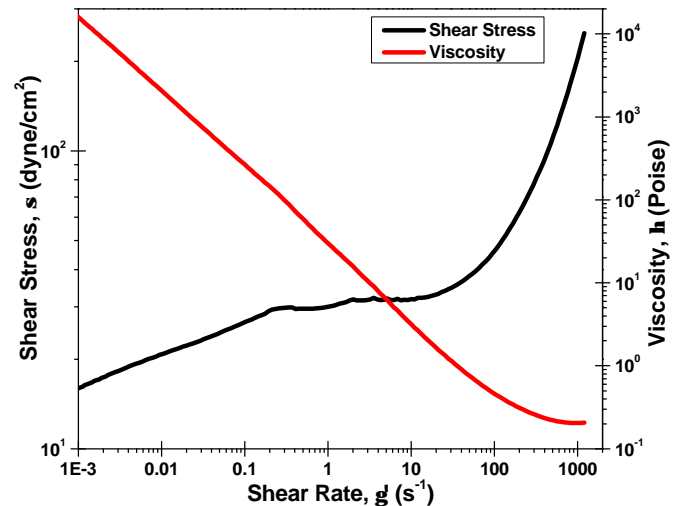
Figure 9   Controlled rate flow curve at 120°F for Fluid #4, demonstrating behavior similar to that predicted by the Mendes-Dutra model.

curve for Fluid #2 inflects and begins to increase at low strain rates, resembling the prediction of the thixotropy model when structural growth becomes significant. This type of behavior could be expected, given the structural growth at low rates exhibited in Figure 5. The behavior of Fluid #4, however, resembles the Mendes and Dutra prediction, with a yield stress plateau and a lower flow region. Unlike the Mendes and Dutra prediction, however, the region below the yield stress plateau is not a Newtonian regime. Fluid #4 exhibited strong thixotropy (Figure 4) but appeared to have a more fragile gel structure than did Fluid #2; this difference in the durability of the gel structure is likely what gives rise to the differences in observed behavior between the two fluids.

A comparison of the fits of the standard models to the controlled strain rate flow curves for Fluids #2 and #4 are presented in Figure 10 and Figure 11. Only models for which solutions could be found are presented. For Fluid #2 (Figure 10) we find that none of the standard models predict the stress inflection at low rates which was observed experimentally. Of the four models shown, the Bingham plastic and Carreau models presented the worst fits, badly missing the behavior in the shear-thinning region; this is despite the qualitatively good fit for a six-point fit from the Model 35A viscometry (Figure 7). The Herschel-Bulkley and Casson models produced very similar fits, modeling the shear-thinning region well but not the shear inflection at low rates.

For Fluid #4 (Figure 11), we again see that the Bingham plastic model poorly fits the expanded data. Additionally, the Herschel-Bulkley and Casson models again fit the shear-thinning region but not the experimentally observed yield stress plateau and lower flow regions. However, unlike with Fluid #2, the Carreau and Cross models provide reasonable fits of the data, modeling the upper shear-thinning region well while qualitatively predicting the yield stress plateau and lower flow regions.
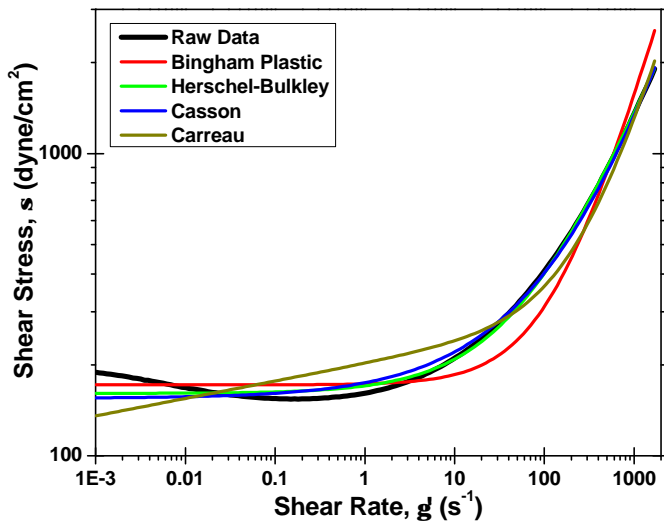
Figure 10 Comparison of standard model fits to the flow curve for Fluid #2, from controlled rate testing at 120°F.
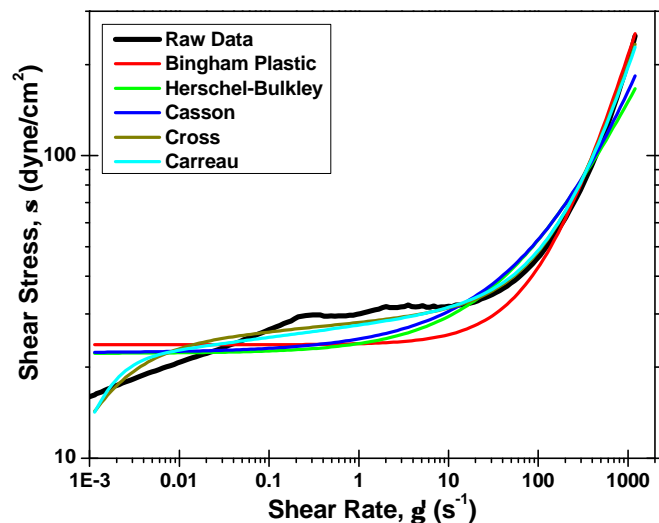

Figure 11 Comparison of standard model fits to the flow curve for Fluid #4, from controlled rate testing at 120°F.

Very different flow curves for these fluids were observed when tested in controlled stress sweeps (see Figure 12 and Figure 14). The first difference is the variability in the flow curves of each fluid when the equilibration time per data point is increased. As the fluid is allowed additional time at each stress to reach a steady state between structural growth and flow, the strain rate at that stress decreases. The result is a curve that strongly resembles that predicted by Mendes and Dutra. The equilibration time required is less at higher shear stresses (usually those which result in rates greater than ~100 s^{-1}), but at lower stresses – those near the yield stress plateau – a difference in resultant strain rates of five orders of magnitude can be observed. In some cases, as in Fluid #2, the

necessary equilibration time is relatively long (around 100-seconds per point), while in the case of Fluid #4 the time required per data point is relatively short (around 10-seconds per point). For both Fluid #2 and #4, the Mendes-Dutra model fit the experimental data at equilibrium with the exception of the region below the yield stress plateau, where the model predicts Newtonian behavior while experimental data suggests shear-thinning.
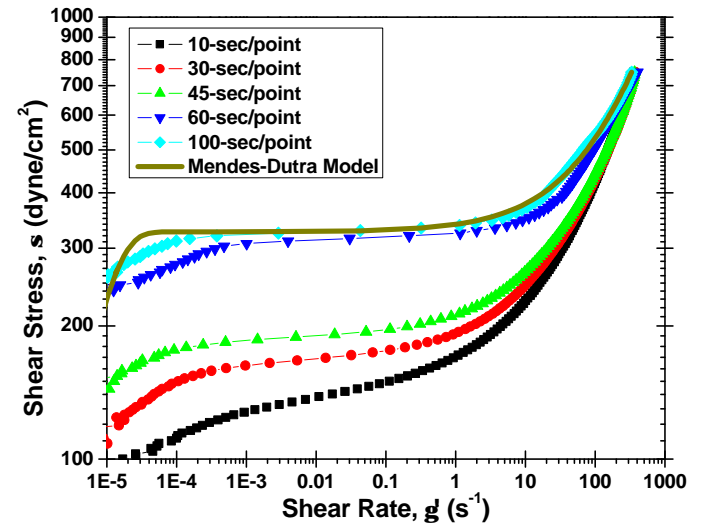

Figure 12 Controlled stress flow curves at 120°F, with varying equilibration times for each data point, for Fluid #2, demonstrating behavior similar to that predicted by the Mendes-Dutra model.

Figure 13 Controlled stress flow curves at 120°F, with varying equilibration times for each data point, for Fluid #4, demonstrating behavior similar to that predicted by the Mendes-Dutra model.
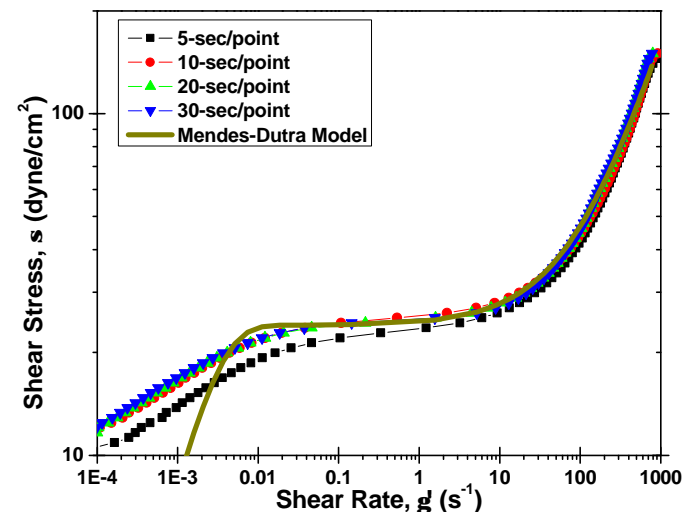
A comparison of the standard models to the Mendes-Dutra fit for a controlled shear stress test of Fluid #2, allowing 100-seconds per point, is presented in Figure 14. As was noted

from fitting the data from controlled rate tests, the standard models best fit the experimental data in the shear-thinning region. The yield stress plateau and lower flow region are poorly fit by the standard models. The Mendes-Dutra model provides a noticeably better fit for the extended data sets than do any of the standard models.
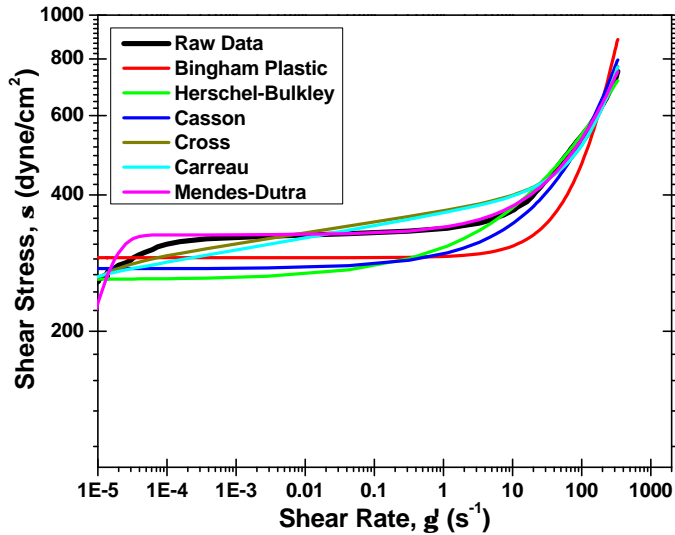

Figure 14 Controlled stress curve at 120°F for Fluid #2, at 100-seconds per data point, with fits from the standard models and the Mendes-Dutra model.

A comparison of experimentally determined yield stresses and Model 35A gel strengths with model predictions is presented in Table 6. Gel strengths were determined as described in Test Methods A and B (Table 4) and direct yield stress measurements were conducted under controlled stress conditions, with the applied stress increased until flow was observed. Both gel strength and direct yield stress tests were conducted after preshearing and allowing a 10-second, 10-minute, or 30-minute gel growth period. Model predicted yield stresses were based on fitting of the models to extended strain rate sweeps.

Differences were observed in the gel strength results from Test Method A and Test Method B. For Fluids #1, #3, and #4, relatively little difference was observed between results of the two test methods (a difference of 5.1-dyne/cm^2 is equivalent to a difference of one dial reading on a Model 35A and is considered within experimental error of the equipment). When Fluid #2 was tested by Method B, though, the resultant gel strengths were significantly lower than those observed from Test Method A. This would indicate that for Fluid #2, Test Method A, which resembles a more time-constrained test allowing minimal shearing between gel strength measurements, residual structure that had not been broken down remained and resulted in elevated gel strengths. By using longer shear times between the gel measurements, this structure was broken down and lower values were obtained.

The results of direct yield stress measurements with varying gel growth periods showed greater variation in results

Table 6 Measured and model-predicted yield stresses for the four test fluids (in dyne/cm^2). Fluids were tested at 120°F in ascending stress sweeps and also by API gel strength tests after various gel growth periods. Predicted yield stress values were obtained from fitting models to extended strain rate sweeps.

dyne/cm^2	Fluid #1	Fluid #2	Fluid #3	Fluid #4
Direct Yield Stress Measurements				
10-second gel period	10.4	208.6	42.1	50.9
10-minute gel period	26.8	249.6	49.2	55.4
30-minute gel period	40.3	473.1	50.4	51.1
Model 35 Gel Strengths, Test Method A				
10-second gel period	34.2	120.0	29.7	40.2
10-minute gel period	52.6	237.0	61.6	69.8
30-minute gel period	58.2	347.3	68.8	76.3
Model 35 Gel Strengths, Test Method B				
10-second gel period	36.8	104.7	32.8	36.9
10-minute gel period	57.7	215.0	64.3	67.4
30-minute gel period	68.9	300.3	73.3	80.3
Model Predicted Yield Stresses				
Bingham Plastic	29.9	171.7	21.9	23.7
Herschel-Bulkley	30.7	161	14.3	22.2
Casson	29.6	155	19.3	22.3
Mendes-Dutra	26.2	326.5	18	24

from 10-second to 30-minute gel periods. In general, with the exception of Fluid #2, the direct yield stress results were lower than the measured gel strengths; this is to be expected as the API gel strength is less a measure of yield stress than it is a measure of shear stress upon inception of flow at an imposed strain rate. The two water-based fluids, Fluids #1 and #2, exhibited more progressive gel strengths and yield stresses than did the oil-based fluids, Fluids #3 and #4. Among the model-predicted yield stresses, those from the Bingham plastic, Herschel-Bulkley, and Casson models give qualitatively similar results while the Mendes-Dutra model produces a slightly lower or higher prediction for most of the fluids. In addition, for Fluids #1 and #2 the model-predicted yield stresses are similar to the results of the direct yield stress

measurements taken after a 10-minute gel growth period, indicating that they provide a reasonable approximation of the fluids yield stress. For Fluids #3 and #4, however, the model-predicted yield stresses were approximately half the directly measured yield stresses.

Conclusions

- Oilfield drilling fluids exhibit varying degrees of thixotropy. The effects of fluid thixotropy impact measured properties through the interaction of dynamic growth and destruction of structure within the fluid.
- Drilling fluids also exhibit yield stress behavior, exhibiting yield stress plateaus below which flow is likely unstable or non-uniform.
- Measured flow properties in drilling fluids are highly dependant on the test employed. Results may be effected by the time allowed for measurements to be taken and by the method in which the test is carried out (i.e. strain control verses stress control testing).
- Both standard and more recent models have a limited utility in describing fluid behavior. No single model did a good job in predicting the behavior of all the test fluids. Additionally, the modeled yield stress was not always comparable with the experimentally observed yield stress.
- There is significant room for improvement in the understanding of the mixed thixotropic and yielding natures of drilling fluids and in the definition of the observed fluid behavior.

Nomenclature

$\dot{g}$ = strain (or shear) rate, s^{-1} or Hz

s = shear stress, $dyne/cm^2$ or $lb/100\ ft^2$

h = viscosity, Poise or cP

s_0 = yield stress, $dyne/cm^2$ or $lb/100\ ft^2$

h_0 = zero-shear viscosity, Poise or cP

$h_\yen$ = upper-Newtonian viscosity, Poise or cP

h_p = plastic viscosity, Poise or cP

References

1. Jachnik, Richard: "Drilling Fluid Thixotropy and Relevance," *Ann. Trans. Nordic Rheo. Society* v. 13 (2005).
2. Møller, Peder C.F., Jan Mewis, and Daniel Bonn: "Yield Stress and thixotropy: on the difficulty of measuring yield stress in practice," *Soft Matter* v. 2 (2006), 274-283.
3. Potanin, Andrei: "Thixotropy and rheopexy of aggregated dispersions with wetting polymer," *J. Rheo.* v. 48 (Nov/Dec 2004), 1279-1293.
4. Davison, J., Clary, S., Saasen, A., Allouche, M., Bodin, D., and Nguyen, V-A.: "Rheology of Various Drilling Fluid Systems Under Deepwater Drilling Conditions and the Importance of Accurate Predictions of Downhole Fluid Hydraulics" SPE 56632, SPE Annual Technical Conference, Houston, Oct. 3-6, 1999.
5. Mendes, Paulo R. Souza and Eduardo S. S. Dutra: "A Viscosity Function for Viscoplastic Liquids," *An. Trans. Nordic Rheo. Soc.* v. 12 (2004), 183-188.